Supplementary Information for

Low reflectance of carbon nanotube and nanoscrolls based thin film coatings:

a case study

Sonia Saini[1, 2], S Reshmi [3] Girish M. Gouda[2], Ajith Kumar S[2], Sriram K V[2] and K

Bhattacharjee[1, 3, *]

[1]Indian Institution of Space Science and Technology (IIST), Thiruvanthapuram, 695 547, India

[2]Laboratory for Electro-Optics Systems (LEOS), Indian Space Research Organization (ISRO), Bengaluru, 560 058, India

[3]Institute of Physics, Sachivalaya Marg, Bhubaneswar 751005, Odisha, India

*Corresponding author: kbhattacharjee@iopb.res.in; kuntala.iopb@gmail.com
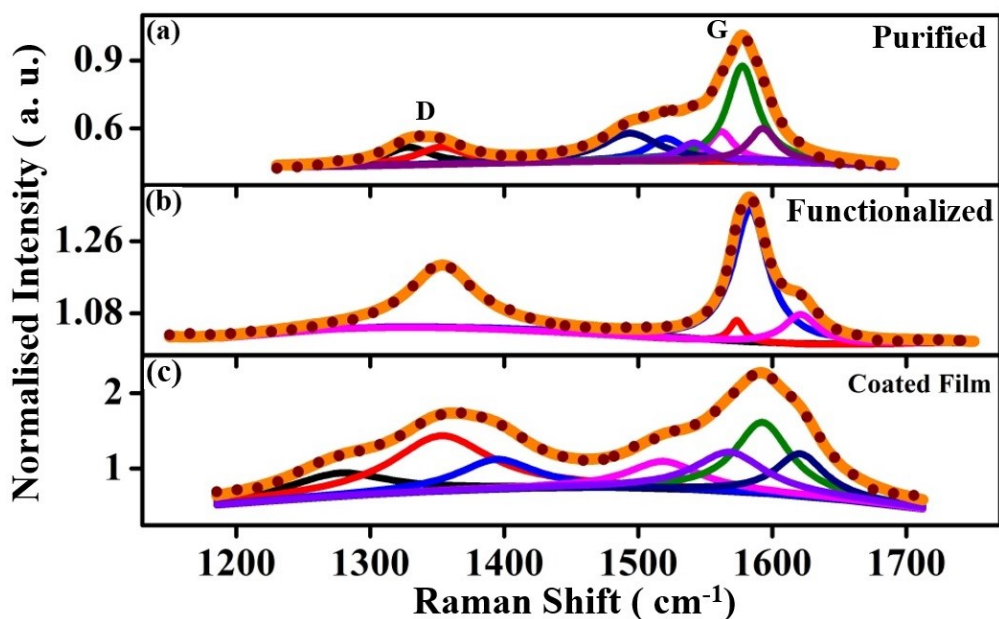
I. Analysis on Raman D, G and 2D Bands:

Figure S1. Peak fit of Raman D and G band of purified, functionalized and coated SWCNT film using Lorentz profiles. *The intensity of the spectra is normalized w.r.t. the G peak of the purified data.*

Defect induced Raman D and G bands of purified, functionalized, and coated film samples are shown in Figure S1. The bands are approximated using Lorentz oscillators. Fitted D bands exhibit two (1328.45 and 1352.85 cm^{-1}), one (1354 cm^{-1}) and three (1277.35, 1352.83, 1394.55 cm^{-1}) components [Figure S1] respectively for the purified, functionalized, and coated film. G band which is the vibration of two unlike C atoms in the graphite unit cell is usually comprised of two peak features, a low-frequency G- and a high-frequency G+ arising from the confinement of phonon wave vector. While G- corresponds to transverse optical (TO) phonon which is the vibration of C atoms along the nanotube circumferential direction, G+ is associated with a longitudinal optical (LO) phonon signifying vibration along the nanotube axis [1]. The line shape of the G band is very significant where a narrow symmetric profile observed for each G mode corresponds to chiral semiconducting tubes and a broad softened G- associated with a narrow G+ is accounted for chiral metallic tubes. We find the signature of asymmetric G bands [Figure S1] which exhibit multiple contributions after fitting. Group theory anticipates six Raman active modes with two each of A (A^1_g), E^1 [(E^1_g) and (E_{2g})] within the tangential G band of SWCNTs [2]. In our data, six Lorentz oscillators peaking at 1493.81, 1520.79, 1541.96, 1561.88, 1577.67, and 1592.91 cm^{-1} respectively provide the best fit of the G feature for the purified sample [Figure S1]. Deconvoluted G spectrum of functionalized sample exhibits three Lorentz components at 1573.55, 1583.68, 1621.23 cm^{-1}, while the coated film shows the Lorentz profiles peaking at 1518.96, 1568.29, 1592.68, 1620.84 cm^{-1}. These Lorentz approximations yield COD values, 0.9961, 0.9969, and 0.9977 for the purified, functionalized and coated samples respectively which show the precission of our fit.
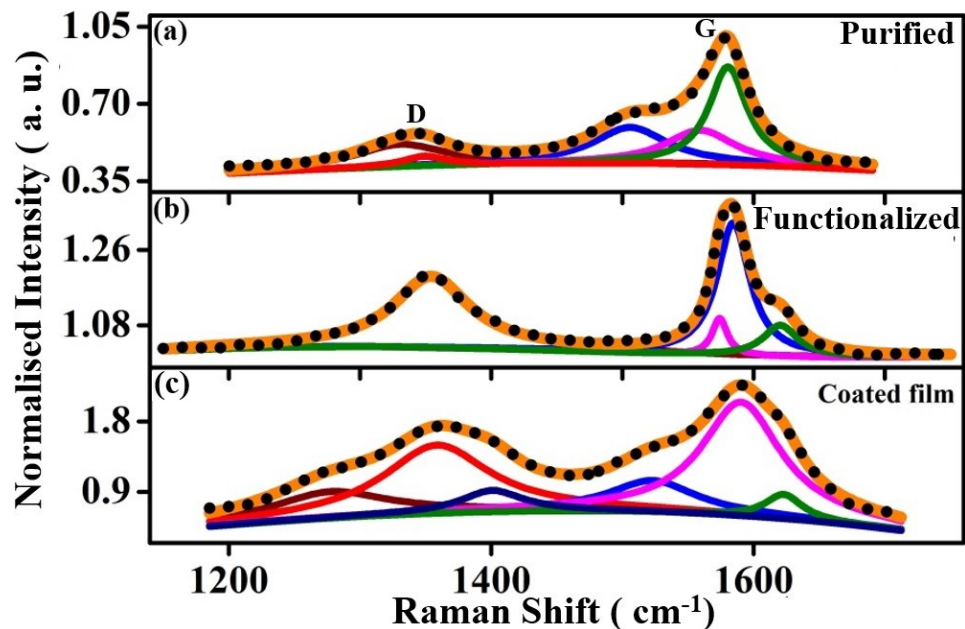
Figure S2. Peak fit of Raman D and G band of purified, functionalized and coated film using a combination of Lorentz and BWF line shapes. *The intensity of the spectra is normalized w.r.t. the G peak of the purified data.*

Our attempt to approximate G bands by considering the combination of Breit Wigner Fano (BWF) [Figure S2] and Lorentz line shapes have yielded a very low coupling strength parameter (phonon interaction with the continuum of states), $1/q \approx 0$ (< 0.007 for the coated film, while for purified and functionalized cases, $1/q$ is of the order of 10^{-6} and 10^{-7} respectively) which is a clear indication that metallic tubes are not in resonance with 2.33 eV laser excitation energy used here.
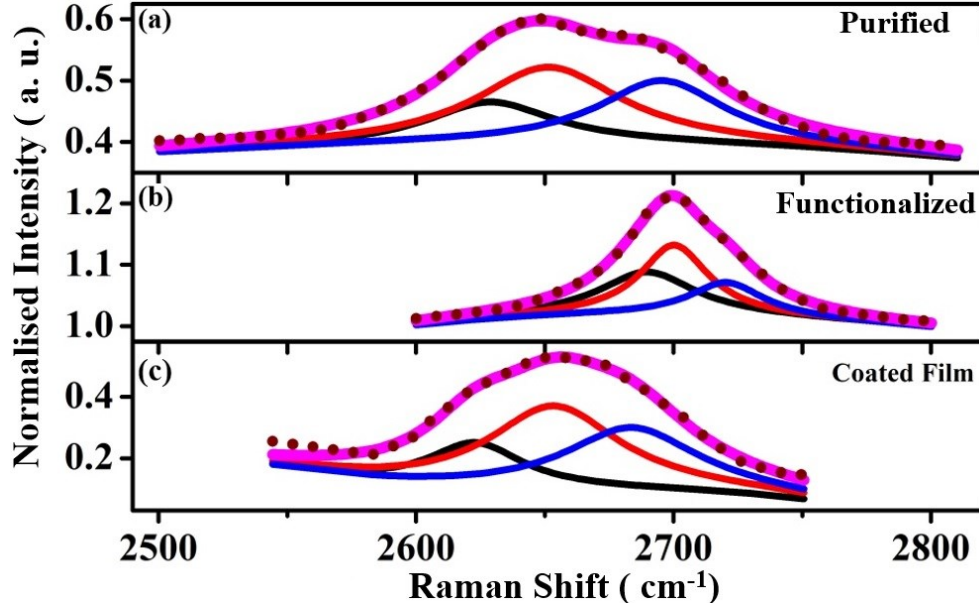
Figure S3. Lorentz approximated Raman 2D band of purified, functionalized, and coated film. *The intensity of the spectra is normalized w.r.t. the G peak of the purified data.*

Figure S3 shows the emergence of 2D or G' band in the respective Raman spectra. 2D, an overtone of D, is due to second-order processes of self-annihilating pair of phonons near the K-point of the zone boundary. This does not require the presence of any defect state to be activated. Each 2D band was well approximated by considering three Lorentz contours [3]. The most intense 2D center peak is situated at 2651.3, 2700.3, and 2653.56 cm^{-1} for the purified, functionalized and coated film respectively [Figure S3]. These center peaks could be associated with single-layer graphene in sample [3]. The low (2628.7, 2689.7, 2623 cm^{-1}) and the high (2695.76, 2720.55, 2683.9 cm^{-1}) frequency peak components on both sides of the main center peak could be assigned to double electron-phonon resonance activities in the samples giving rise to different resonant conditions for resonances with different van Hove Singularities [3].
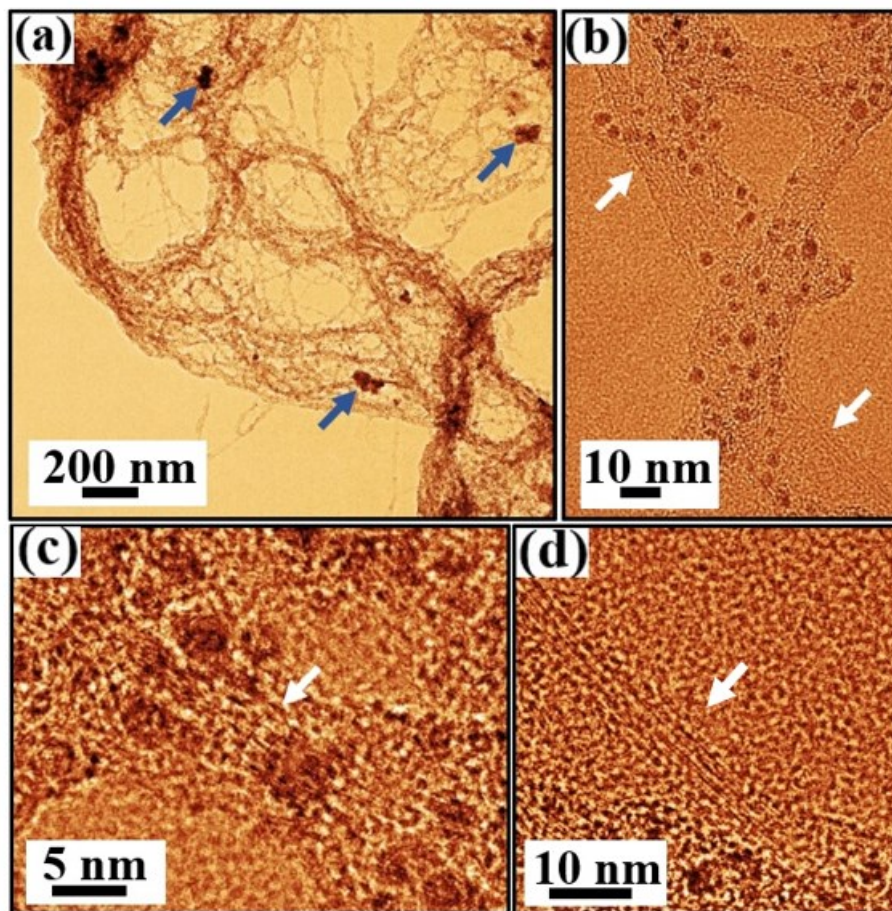
II. SWCNT/MWCNT TEM analysis.

Figure S4. TEM micrographs obtained from the as-prepared SWCNT sample. (a) Shows the large area image with bundled networks of SWCNTs. Amorphous carbonaceous particles are marked in (a) using arrows. (b) (c) and (d) show clear evidence of SWCNTs (marked with white arrows) within the bundled network. Presence of metal nanoparticles are observed as dark spots in (b-d).

We have discussed about Figure S4 in the main text of the manuscript.
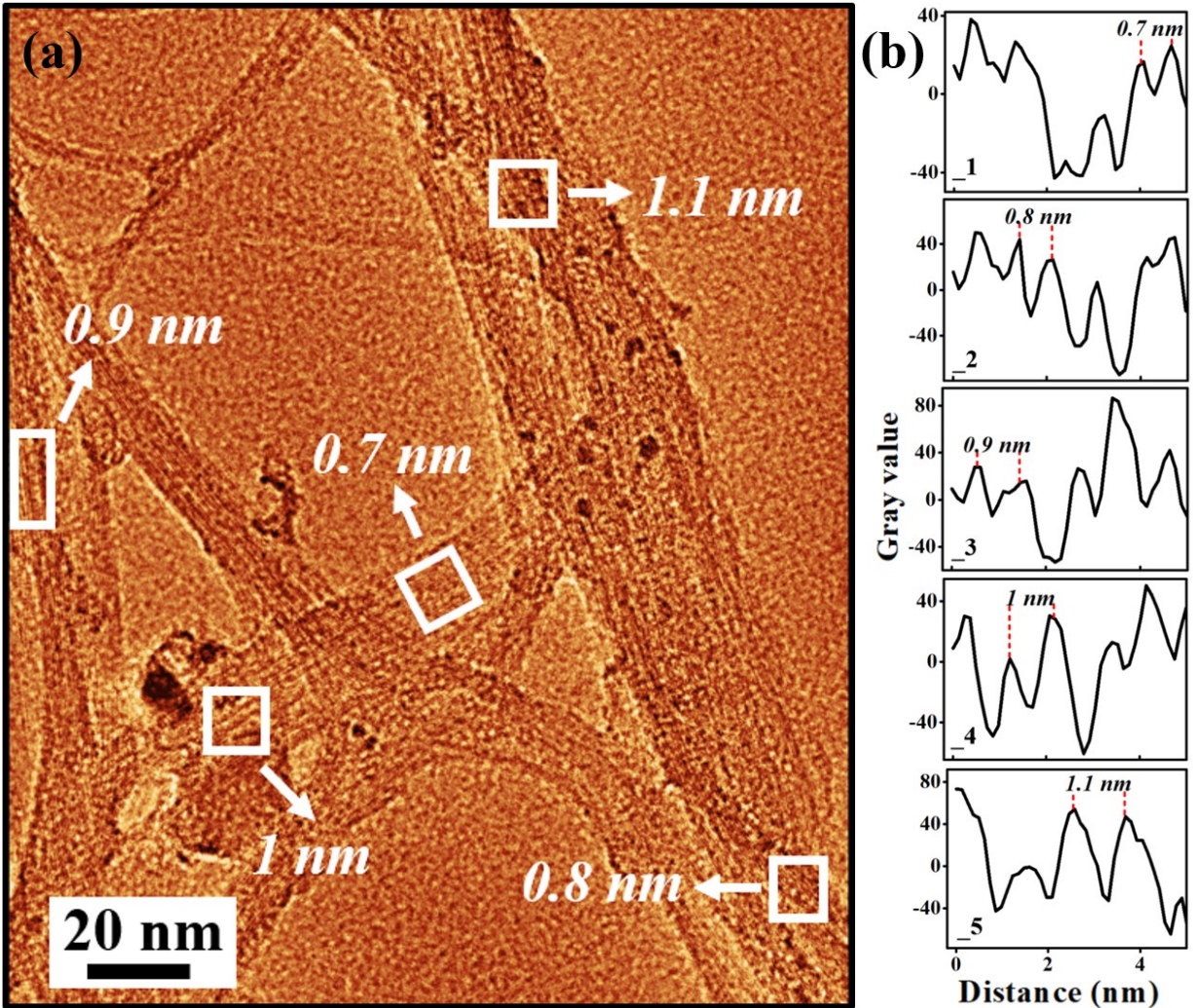
Figure S5. (a) TEM image showing SWCNT strands of varying diameters. The regions of different diameter periodicities are marked using white rectangles on the image. (b) Shows the line profiles taken across each such rectangular region. Diameter periodicity of the SWCNT bundles within the rectangles is marked in the profiles.

Figure S5 shows the TEM image of the purified sample consisting of nanotube bundles. The SWCNTs constituting the bundles have varying diameters. The diameter is estimated using Gwyddion software. The line profile taken across a bundle is averaged w.r.t the number of nanotubes (represented by peaks in the profiles) to obtain an average diameter. We have observed a diameter periodicity ranging from 0.7nm to 1.1 nm in the purified sample.
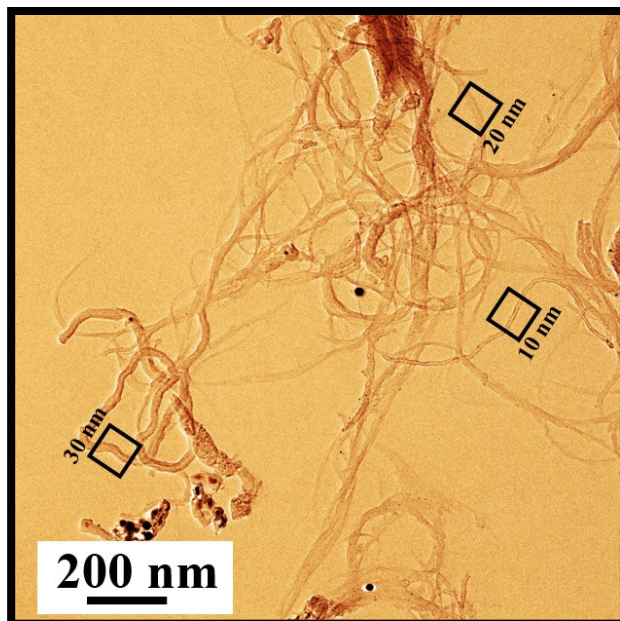
Figure S6. TEM image of the purified sample showing the presence of MWCNTs with varying diameters (marked within black squares)

A similar method is followed to investigate the MWCNT diameters in the purified sample. Figure S6 shows the TEM image from the purified sample which consists of MWCNTs with a diameter distribution ranging from 10 to 30 nm. The regions with MWCNTs of diameter 10, 20, and 30 nm are marked by black squares.
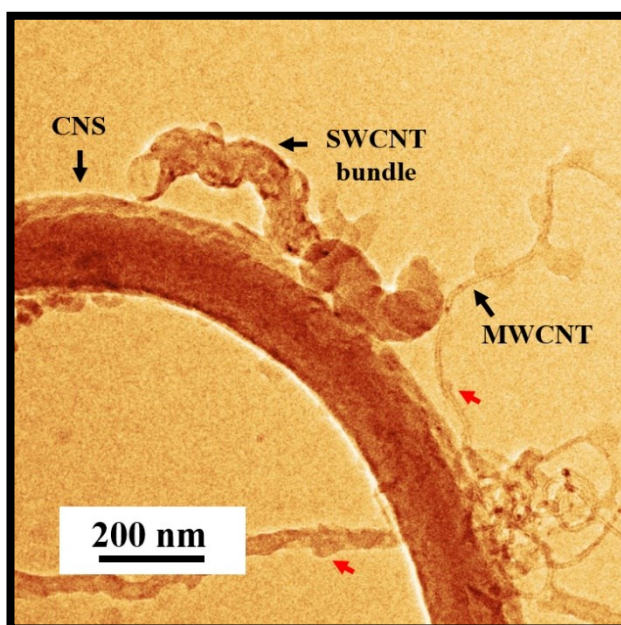
Figure S7. The presence of SWCNT bundles, MWCNT, and CNS in the functionalized sample is marked with black arrows. The attachment of the functional groups is visible as protrusions on the walls of the nanotubes and nanoscroslls (marked with red arrows)

Figure S7 shows the TEM image of the functionalized sample. After functionalization, we see a direct evidence of the functional groups attached on the walls of the tubes and scrolls. In figure S7, we have marked such attachments with red arrows. The sample after the purification as well as functionalization process consists of MWCNT as well as CNS in addition to the SWCNT bundles. All these are marked and labeled in figure S7.

References

1   M. S. Dresselhaus, G. Dresselhaus, R. Saito and A. Jorio, *Phys. Rep.*, 2005, **409**, 47–99.

2   S. D. M. Brown, A. Jorio, P. Corio, M. S. Dresselhaus, G. Dresselhaus, R. Saito and K. Kneipp, *Phys. Rev. B*, 2001, **63**, 155414.

3   Y. Stubrov, A. Nikolenko, V. Gubanov and V. Strelchuk, *Nanoscale Res. Lett.*, 2016, **11**, 2.